

Improved Inactivation Effect of Bacteria: Fabrication of Mesoporous Anatase Films with Fine Ag Nanoparticles Prepared by Coaxial Vacuum Arc Deposition

Hamid Oveisi,^{1,2} Simin Rahighi,³ Xiangfen Jiang,^{1,4} Yoshiaki Agawa,⁵
Ali Beitollahi,² Soichi Wakatsuki,³ and Yusuke Yamauchi^{*1,4,6}

¹World Premier International (WPI) Research Center for Materials Nanoarchitectonics (MANA),
National Institute for Materials Science (NIMS), 1-1 Namiki, Tsukuba, Ibaraki 305-0044

²Center of Excellence for Advanced Material Processing, School of Metallurgy and Materials Engineering,
Iran University of Science and Technology (IUST), Narmak, Tehran 1684613114, Iran

³Structural Biology Research Center, High Energy Accelerator Research Organization (KEK),
1-1 Oho, Tsukuba, Ibaraki 305-0801

⁴Faculty of Science and Engineering, Waseda University, 3-4-1 Okubo, Shinjuku-ku, Tokyo 169-8555

⁵ULVAC-RIKO, Inc., 1-9-19 Hakusan, Midori-ku, Yokohama, Kanagawa 226-0006

⁶Precursory Research for Embryonic Science and Technology (PRESTO), Japan Science and Technology Agency (JST),
4-1-8 Honcho, Kawaguchi, Saitama 332-0012

(Received January 20, 2011; CL-110048; E-mail: Yamauchi.Yusuke@nims.go.jp)

We realize ultrarapid inactivation of bacteria by modifying fine Ag nanoparticles with uniform size on mesoporous anatase films with high surface areas.

Diseases caused by bacteria, viruses, fungi, and other parasites are major causes of deaths, disabilities, and social and economic disruption for millions of people. Infections acquired in hospital or in the course of medical treatment present a serious burden for patients and the health systems. Over 9.5 million people die each year due to infectious diseases in developing countries. There are many kinds of disease (e.g., listeriosis and strep throat) which can be caused by bacteria contamination of the environment. *Escherichia coli* (*E. coli*), gonococcus, salmonella, staphylococcus bacteria, streptococcus, and typhoid bacillus, are well known as common bacteria. For instance, enterohemorrhagic *E. coli* is very dangerous bacteria which can cause serious diarrhea.

Therefore, the most urgent requirement for humans is to prevent these diseases by applying materials that are capable of killing or inactivating the causative bacteria. The development of new materials with high antibacterial properties has long been the goal of medical science. Up to now, the most commonly used antibacterial agents are extremely toxic to the environment, and their residues can react with the environment with detrimental effects. Although currently new types of antibacterial film with enhanced activity have been fabricated by mixing with complex polymer-based materials or using special equipment such as CVD (chemical vapor deposition), their fabrication is still not simple.¹

Robust inorganic materials have received more recognition in the antibacterial market and photocatalytic products, because of their high heat resistance and long life expectancy. Especially, titanium dioxide (titania, TiO₂) has been recognized as the most familiar substance for widespread environmental applications,² because of its biological and chemical inertness, strong oxidizing power, nontoxicity, and long-term stability. Nowadays, titania nanomaterials with various morphologies have been used for wide applications such as a water treatment, air purification, hazardous waste remediation, environmental purification, and deactivation of bacteria.³

The antibacterial activity of titania strongly depends on its crystal structure, surface area, and surface morphology. Crystallized anatase nanoparticles (e.g., Degussa P-25) show excellent photocatalytic activity which offers potentially a facile and cheap method to clean the environment from pollutant traces as well as from biological organisms such as bacteria and viruses. Mesoporous anatase with extremely high surface area can provide a higher amount of hydroxyl radical which can increase the antibacterial activity compared to commercially available products.⁴ In particular, the thin mesoporous anatase films have open mesopores on the surface, providing accessible diffusion pathways for the generated radicals.^{4c} In our previous study, excellent inactivation of bacteria was realized by tuning several significant factors such as surface area, anatase crystallinity, and surface morphology.^{4c} After only 20 min of UV irradiation, more than 98% of *E. coli* was inactivated, which was the highest activity among all the titania-based materials reported previously.

To further enhance the antibacterial properties, here we focus on modification of metal nanoparticles to mesoporous anatase films. Previous work on semiconductor–metal composites have revealed that deposition of metal onto semiconductor enhances efficiency of photocatalytic reaction.⁵ The metal nanoparticles (e.g., Ag, Au, and Pt) deposited on semiconductor substances can efficiently promote electron–hole separation.⁵ Among several metal nanoparticles, Ag is the most popular metal and has been commonly used to modify TiO₂ surfaces. In this communication, we succeeded in drastically enhancing antibacterial activity by uniformly depositing Ag nanoparticles on mesoporous anatase films. Surprisingly, mesoporous titania films with Ag nanoparticles can inactivate around 90% *E. coli* bacteria within only 2 min under UV irradiation. Our process based on sol–gel chemistry is very simple, low-cost, and can offer high turnover on an industrial scale, and has a potential of becoming a key technology for solving current societal problems.

In this study, mesoporous anatase films were prepared by spin-coating precursor solution followed by calcination at 450 °C. Through the previous systematic adjustment,^{4c} the calcination temperature was fixed to be 450 °C.⁶ Then, Ag nanoparticles were deposited onto the films by using coaxial pulsed vacuum arc discharge deposition (APD).⁷ The amounts of the deposited Ag were varied from 0 to 2.77×10^{-5} , $1.39 \times$

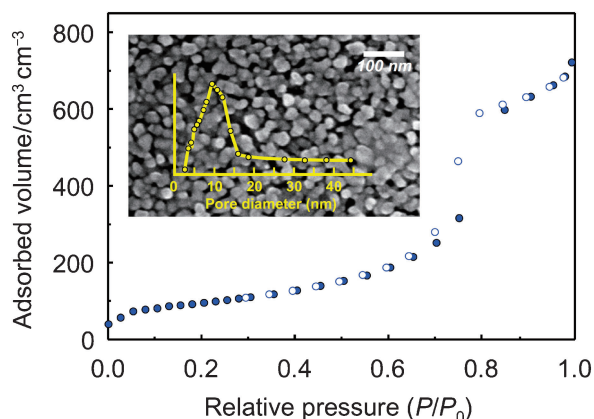


Figure 1. Nitrogen adsorption–desorption isotherm of mesoporous anatase film (●: adsorption, ○: desorption). SEM image of the film surface and the mesopore size distribution are also shown as an inset image.

10^{-4} , and 5.54×10^{-4} mg cm $^{-2}$ by changing pulse counts (0, 10, 50, and 200 pulse). Hereafter, these Ag-modified mesoporous anatase films were abbreviated as **meso-0Ag**, **meso-10Ag**, **meso-50Ag**, and **meso-200Ag**. The experimental details are given in Supporting Information.⁸

Before investigation of antibacterial toxicity, we carefully characterized the mesoporous anatase films with Ag nanoparticles. Typical scanning electron microscopic (SEM) images of mesoporous anatase before and after the Ag deposition are shown in Figures 1 (inset) and S1,⁸ respectively. The anatase films showed continuous surfaces without any cracks. Mesoporous structures were observed, which was detected by N₂ gas adsorption–desorption isotherms (Figure 1). The average pore size was around 10 nm. Wide-angle XRD patterns for all the anatase films with different amounts of Ag showed a broad diffraction peak at $2\theta = 25^\circ$ which are assignable to anatase phase (Figure S2⁸). **Meso-10Ag** and **meso-50Ag** films do not exhibit peaks related to Ag metal, indicating that the Ag nanoparticles were finely dispersed on the film surface without agglomeration of the silver particles. Even after the Ag deposition, the open mesopores still existed in the film surface (data not shown). However, when the pulse numbers increased to 200 counts, Ag peaks at higher angle ($2\theta = 38^\circ$) appeared, due to the formation of large-sized Ag nanoparticles (Figure S2⁸). As shown in Figure S1,⁸ it was clearly seen that agglomeration of large-sized Ag nanoparticles occurred on the surface of the mesoporous film.

In general, particle sizes of Ag deposited on TiO₂ surfaces have great effect on the antibacterial properties.^{5c} To quantitatively evaluate the sizes of the deposited Ag nanoparticles, the particle size distributions were calculated by direct TEM observation (Figure S3⁸). The average sizes were 3.7 (for **meso-10Ag**), 3.9 (for **meso-50Ag**), and 5.6 nm (for **meso-200Ag**), respectively. The Ag nanoparticles for **meso-10Ag** centralize at a diameter of 3.2 nm, although only a few large nanoparticles (about 6 nm in diameter) were observed. Thus, by using APD, uniformly sized nanoparticles can be formed on the film surface.⁷ However, in the case of **meso-50Ag** and **meso-200Ag**, the particle size distribution showed two peak regions. For **meso-200Ag**, this trend became much more obvious.

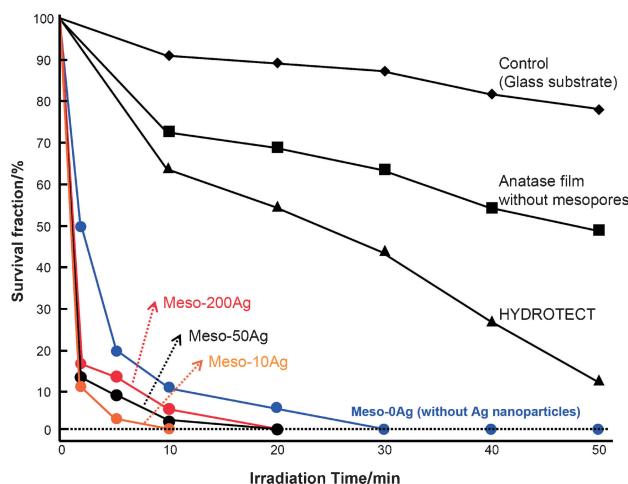


Figure 2. Antibacterial properties of mesoporous anatase films with different amounts of Ag nanoparticles (**meso-0Ag**, **meso-10Ag**, **meso-50Ag**, and **meso-200Ag**). The fraction of surviving *E. coli* cells as a function of the UV irradiation time. Glass substrate, anatase film without mesopores, and a commercially available photocatalyst are also compared.

Although Ag nanoparticles less than 5 nm are predominately formed for all the samples, the second particle size distribution shifted to larger-size, thereby increasing the average particle sizes. With the increase of the applied pulse accounts, the Ag nanoparticles are thought to aggregate to form larger particles. The selected-area electron diffraction (ED) patterns showed rings assignable to Ag *fcc* structure (data not shown). X-ray photoelectron spectroscopy (XPS) was also utilized to analyze electronic states of the deposited Ag nanoparticles. Both Ti 2p and Ag 3d peaks appeared on all the samples (Figure S4⁸). The Ag 3d_{5/2} region could be further deconvoluted into three peaks locating at 368.2, 367.7, and 367.3 eV, which corresponded to metallic Ag(0), oxidized Ag(I) (AgO₂), and oxidized Ag(II) (AgO), respectively (Figure S5⁸). As a result, the relative atom ratios of metallic Ag(0) (Ag(0)/(Ag(0) + Ag(I) + Ag(II))) were 52% (for **meso-10Ag**), 33% (for **meso-50Ag**), and 24% (for **meso-200Ag**), respectively.

The antibacterial activity of the mesoporous anatase films with Ag nanoparticles was examined. The details of experiments are described in Supporting Information.⁸ Here, we used *E. coli* (BL21, DE3), a gram-negative bacterium, as model bacteria. Luria broth (LB) and agar were used as media for culturing *E. coli*. The cell suspensions used for antibacterial activity contained ca. 10⁸ colony-forming units (CFU)/mL. The cell suspension was dripped onto the films and UV irradiation was applied. After the irradiation, the surface of each film was washed with PBS (phosphate buffer saline). Each washed solution was spread on LB agar and incubated before counting the colonies. The results are summarized as the percentage of survival fraction (%) as a function of exposure time (min) using the following equation: (CFU after exposure/CFU before exposure) \times 100.

Figure 2 shows photocatalytic disinfection by mesoporous anatase films with and without the Ag nanoparticles. For comparison, we also tested nonporous anatase film (calcined at 450 °C) and commercially available photocatalyst (HYDROTECT, TOTO LTD.⁹) whose photocatalytic activity is

superior to P-25 nanoparticles. The nonporous anatase film showed about 50% inactivation of *E. coli* by 50 min UV irradiation. In the case of HYDROTECT photocatalyst, almost 87% of *E. coli* cells were inactivated after 50 min of UV irradiation. On the other hand, mesoporous anatase films with high surface area showed more than 90% inactivation of *E. coli* by only 10 min of UV irradiation. The antibacterial properties of mesoporous anatase films with different amounts of Ag (**meso-10Ag**, **meso-50Ag**, and **meso-200Ag**) are also shown in Figure 2. The results showed that the disinfection by all three types of Ag-modified films dramatically increased in comparison with mesoporous anatase film without Ag nanoparticles (**meso-0Ag**). The highest antibacterial efficiency was observed for **meso-10Ag** in a manner that 98% reduction in the number of cells occurred after only 5 min of UV irradiation. Also, **meso-10Ag** could inactivate 100% of *E. coli* after 10 min. To the best of our knowledge, this is the highest among all of the previous work.^{1,4a,4c} In the other films, after 5 min irradiation, 90% and 85% reduction in the number of cells occurred for **meso-50Ag** and **meso-200Ag**, respectively. These results confirmed that the antibacterial toxicity was dramatically enhanced by modifying the Ag nanoparticles.

In the photocatalytic oxidation of bacteria, the UV light irradiation produces a pair of negative electrons (e^-) and holes (h^+) in the mesoporous anatase films. They are diffused or trapped on/near the film surface. These generate a large number of electrons and holes that are strong reducing and oxidizing agents, respectively, which react with atmospheric water and oxygen. The holes (h^+) can break the water molecules to form hydroxyl radicals ($\bullet OH$), while the electrons (e^-) react with oxygen molecules to form superoxide anions (O_2^-). These free radicals destroy the bacterial cells by oxidizing the organic components in the cell membranes. Mesoporous anatase film with high surface area can generate lots of pairs of negative electrons (e^-) and holes (h^+), thereby dramatically increasing the antibacterial toxicity. However, the electrons (e^-) and holes (h^+) generated from the anatase surface are very unstable and they tend to recombine immediately. The Ag nanoparticles can efficiently promote the electron-hole separation, which can further enhance the reaction efficiency.⁵ The Ag particle sizes deposited on TiO_2 surface showed great effect on the antibacterial properties. Our data demonstrated that the increase of the particle size decreased the deactivation rate. Kamat et al. reported a critical effect of metal nanoparticle sizes on photocatalytic reduction efficiency in TiO_2 -Au composite system.^{5c} With the decrease of the metal nanoparticle sizes, a negative shift in the apparent Fermi level is observed, which is caused by a high degree of electron accumulation. The shift in the Fermi level observed with smaller metal nanoparticles is reflected in the greater photocatalytic reduction efficiency. As another reason, the relative atom ratio of metallic Ag(0) in **meso-10Ag** was much higher than those in **meso-50Ag** and **meso-200Ag**, as detected by XPS analysis (Figure S5⁸). Only the metallic Ag nanoparticles (not oxidized) can better absorb the photoexcited electrons from the anatase, making an effective delay in the electron-hole recombination. Furthermore, in the case of **meso-200Ag**, large Ag nanoparticles were formed on the film surface (Figure S1⁸). Therefore, the large particles might physically prevent rapid diffusion of the reactive radicals to the film surface, decreasing the disinfection efficiency.

In conclusion, we proposed new approaches for practical fabrication of antibacterial materials with high mechanical stability and nontoxicity. In the current industry practices, metal nanoparticles have been prepared by wet impregnation. However, it is not easy to deposit fine metal nanoparticles with fine uniform size onto matrix. In this study, by using a newly developed APD method,⁷ we could successfully coat uniform Ag nanoparticles with effective size onto photoactive mesoporous anatase films prepared by sol-gel techniques. In the future, by tuning sizes and compositions of deposited metal nanoparticles, we anticipate that we can further enhance the antibacterial properties.

References and Notes

- a) Y. Liu, X. Liu, X. Wang, J. Yang, X.-J. Yang, L. Lu, *J. Appl. Polym. Sci.* **2010**, *116*, 2617. b) A. El-Mekawy, S. Hudson, A. El-Baz, H. Hamza, K. El-Halafawy, *J. Appl. Polym. Sci.* **2010**, *116*, 3489. c) J. Mungkalasiri, L. Bedel, F. Emieux, J. Doré, F. N. R. Renaud, C. Sarantopoulos, F. Maury, *Chem. Vap. Deposition* **2010**, *16*, 35. d) K. Vimala, Y. M. Mohan, K. S. Sivudu, K. Varaprasad, S. Ravindra, N. N. Reddy, Y. Padma, B. Sreedhar, K. MohanaRaju, *Colloids Surf., B* **2010**, *76*, 248. e) Y. Inoue, M. Uota, T. Torikai, T. Watari, I. Noda, T. Hotokebuchi, M. Yada, *J. Biomed. Mater. Res., Part A* **2010**, *92A*, 1171. f) F. R. Marciano, L. F. Bonetti, N. S. Da-Silva, E. J. Corat, V. J. Trava-Airoldi, *Synth. Met.* **2009**, *159*, 2167. g) J. Mungkalasiri, L. Bedel, F. Emieux, J. Doré, F. N. R. Renaud, F. Maury, *Surf. Coat. Technol.* **2009**, *204*, 887. h) C. W. H. Dunnill, Z. A. Aiken, A. Kafizas, J. Pratten, M. Wilson, D. J. Morgan, I. P. Parkin, *J. Mater. Chem.* **2009**, *19*, 8747. i) C. W. H. Dunnill, Z. A. Aiken, J. Pratten, M. Wilson, D. J. Morgan, I. P. Parkin, *J. Photochem. Photobiol., A* **2009**, *207*, 244.
- a) A. Fujishima, K. Honda, S. Kikuchi, *Kogyo Kagaku Zasshi* **1969**, *72*, 108. b) A. Fujishima, K. Honda, *Nature* **1972**, *238*, 37.
- a) S. Nagamine, Y. Tanaka, M. Ohshima, *Chem. Lett.* **2009**, *38*, 258. b) S. Li, D. Zhao, J. Zheng, Y. Wan, *Chem. Lett.* **2010**, *39*, 44. c) P. Wang, S.-H. Teng, F.-Q. Tang, *Chem. Lett.* **2010**, *39*, 1140. d) T. Yanagishita, T. Endo, Y. Yamaguchi, K. Nishio, H. Masuda, *Chem. Lett.* **2009**, *38*, 274.
- a) D. S. Kim, S.-Y. Kwak, *Environ. Sci. Technol.* **2009**, *43*, 148. b) T. Kimura, Y. Yamauchi, N. Miyamoto, *Chem.—Eur. J.* **2010**, *16*, 12069. c) H. Oveisi, S. Rahighi, X. Jiang, Y. Nemoto, A. Beitollahi, S. Wakatsuki, Y. Yamauchi, *Chem. Asian J.* **2010**, *5*, 1978.
- a) I. Mikami, S. Aoki, Y. Miura, *Chem. Lett.* **2010**, *39*, 704. b) T. Kimijima, T. Sasaki, M. Nakaya, K. Kanie, A. Muramatsu, *Chem. Lett.* **2010**, *39*, 1080. c) V. Subramanian, E. E. Wolf, P. V. Kamat, *J. Am. Chem. Soc.* **2004**, *126*, 4943. d) A. Dawson, P. V. Kamat, *J. Phys. Chem. B* **2001**, *105*, 960. e) P. V. Kamat, D. Meisel, *C. R. Chim.* **2003**, *6*, 999.
- We investigated antibacterial properties of mesoporous titania films calcined at various temperatures (350, 400, 450, and 500 °C) in our previous work of ref 4c. When mesoporous film was calcined at 450 °C, the framework is successfully crystallized to anatase phase without collapse of mesopores (i.e., with retention of high surface area). This film showed the highest antibacterial property among all the films.
- Y. Agawa, S. Endo, M. Matsuura, Y. Ishii, *Adv. Mater. Res.* **2010**, *123–125*, 1067.
- Supporting Information is available electronically on the CSJ-Journal Web site, <http://www.csj.jp/journals/chem-lett/index.html>.
- http://www.toto.co.jp/docs/hyd_patent_en/.